



## Water Transport Through Nafion 112 Membrane in DMFCs

G. Q. Lu,<sup>a</sup> F. Q. Liu,<sup>b</sup> and Chao-Yang Wang<sup>a,b,\*</sup>

<sup>a</sup>Department of Mechanical and Nuclear Engineering and <sup>b</sup>Department of Materials Science and Engineering, Electrochemical Engine Center, The Pennsylvania State University, University Park, Pennsylvania 16802, USA

Water management has emerged as a significant challenge in portable direct methanol fuel cells, DMFCs. Excessive water crossover through the membrane causes water loss in the anode and flooding in the cathode. We report a novel DMFC design based on Nafion 112 and a cathode gas-diffusion layer coated with a microporous layer. This DMFC operated with ambient air yielded a stable power density of 56 mW/cm<sup>2</sup> at 60°C, while the net water transport coefficient was only 0.64 compared to a typical value of 3 for Nafion 117 membranes. In addition, the fuel efficiency was about 74-92%.  
© 2004 The Electrochemical Society. [DOI: 10.1149/1.1825312] All rights reserved.

Manuscript submitted June 3, 2004; revised manuscript received August 10, 2004. Available electronically November 10, 2004.

The direct methanol fuel cell (DMFC) has the advantages of easy fuel storage, no need for humidification, and simple design. Thus, the DMFC is presently considered a leading contender for portable and micro power.<sup>1-7</sup> To compete with lithium-ion batteries, the first and foremost requirement of a portable DMFC system must be higher energy density in Wh/L.

Constrained by the methanol crossover problem,<sup>8-11</sup> the anode fuel solution has been very dilute, requiring a large amount of water to be carried in the system and thereby reducing the energy content of the fuel mixture. In addition, for each mole of methanol, one mole of water is needed for methanol oxidation at the anode, and roughly 2.5 × 6 mol of water per mole of methanol are dragged through a thick membrane such as Nafion 117 toward the cathode assuming that the electro-osmotic drag coefficient of water is equal to 2.5 per proton.<sup>12</sup> This then causes 16 water molecules to be lost from the anode for every mole of methanol, which corresponds to only 3 M. Water in the anode therefore must be replenished if fuel solutions more concentrated than 3 M are ever to be used. In the cathode 15 water molecules are transported from the anode and three additional water molecules are produced by consuming the six protons generated from oxidation of one methanol. The presence of a large amount of water floods the cathode and reduces its performance. Traditionally, a high cathode gas flow rate (high stoichiometry) is employed to prevent flooding. An external water cooler to condense the cathode effluent must then be used to recycle water back to the anode. This system design not only increases power consumption but also impairs DMFC compactness. The difficult task of removing water from the cathode to avoid severe flooding and supplying water to the anode to make up water loss due to water crossover through the membrane requires innovative water management in a portable DMFC.<sup>13</sup>

Most recently, Blum *et al.*<sup>14</sup> proposed a concept of water-neutral condition under which the anode does not need a water supply and the cell maintains perfect water balance by losing exactly 2 mol of water per mole of methanol consumed. Peled *et al.*<sup>15</sup> further reported experimental data with small or even negative water flux from the anode to the cathode at small current densities using a nanoporous proton-conducting membrane, a compact microporous layer (MPL) on a gas-diffusion layer (GDL) in the cathode, and oxygen at three bars as the oxidant. It was postulated that the hydraulic permeation induced by a hydraulic pressure differential across the membrane can offset the electro-osmotic drag, leading to the net water transport coefficient much smaller than the pure electro-osmotic drag coefficient of ~3 at 60°C.<sup>12</sup>

Based on a recent theory of liquid water transport in polymer electrolyte fuel cells,<sup>16</sup> we have designed a unique membrane-electrode assembly (MEA) structure which utilizes a MPL to build up the hydraulic pressure on the cathode side and a thin membrane

(*i.e.*, Nafion 112) to promote water back-flow under this difference in hydraulic pressure. Such MEAs exhibit extraordinarily low water flux through the polymer membrane. The significance of the experimental work reported here is the fact that commercially available Nafion membranes and MEA materials were used and the cell operated with ambient air without pressurization. Low water flux through the membrane is highly desirable for DMFCs, as the anode does not require an excessive amount of water replenishment. In addition, the cathode is less susceptible to severe flooding and there is less need for water recovery from the cathode effluent, eliminating or shrinking the condenser in a portable system.

### Experimental

**Test apparatus.**—Figure 1 shows a schematic of the experimental setup. The effective area of the DMFC test fixture is 5 cm<sup>2</sup>. A digital pump (Series I digital pump, LabAlliance) with a 0.01-10 mL/min range was used to deliver and control flow rate of aqueous methanol solution. A 2 M methanol solution was employed to test cell performance in this work. A digital mass flow controller (Omega Engineering, Inc) was used to measure and control flow rate of non-heated and nonhumidified air. A digital temperature controller was used to control the electric heater on the cell to maintain desired cell temperature. A water moisture trap containing anhydrous calcium sulfate (W. A. Hammond Drierite Co. LTD) was connected to the exit of the cathode to collect water in the effluent. An electronic load system (BT4, Arbin) in the galvanodynamic polarization mode was used to measure polarization curves at a scan rate of 3 mA/s.

**MEA preparation.**—A catalyst-coated membrane (CCM) was prepared by the decal method.<sup>17</sup> Unsupported Pt/Ru black (HiSPEC 6000, Pt:Ru = 1:1 atomic ratio, Alfa Aesar) and carbon-supported Pt (40% Pt/Vulcan XC72; E-TEK) were used as catalysts for the anode and cathode, respectively. The catalysts were first wetted with a small amount of deionized (DI) water, followed by addition of isopropanol (IPA), ionomer solution (5 wt % Nafion solution, 1100 EW, DuPont), and ethylene glycol. After sufficient magnetic stirring, the ink mixture was treated ultrasonically for 1-2 min and then coated on a Teflon substrate. After being dried for several hours in an oven at 80°C, the coated Teflon film was hot-pressed to a pre-treated Nafion 112 membrane at 125°C and 100 atm for 3 min. The loadings of Pt/Ru and Pt/C in the anode and cathode catalyst layers were 4.8 and 0.9 mg/cm<sup>2</sup>, respectively. The ratio of catalyst to Nafion was maintained at 4:1 (dry weight) for both anode and cathode.

20 wt % wetproofed carbon paper (Toray 090, E-TEK) 0.26 mm thick was used as the anode backing layer. A solution containing Vulcan XC72R carbon black and 40 wt % Teflon (TFE 30, DuPont) was coated on the carbon paper to form a microporous layer (MPL) ~30 μm thick. The gas-diffusion layer (GDL) for the cathode is carbon cloth coated with a microporous layer containing carbon black and Teflon. Figure 2a shows an SEM image of the CCM with the catalyst layer of around 15 μm thickness for both anode and

\* Electrochemical Society Active Member.

<sup>z</sup> E-mail: cxw31@psu.edu

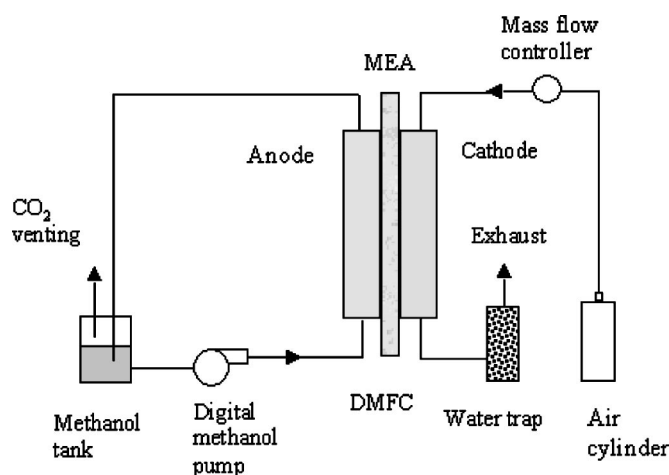


Figure 1. Schematic of the experimental setup.

cathode. Figure 2b shows the shape of water droplets on the surface of the microporous layer of the carbon cloth GDL, indicative of high hydrophobicity.

### Results and Discussion

In the cathode, water is produced by oxygen reduction reaction as well as transported from the aqueous anode due to diffusion and electro-osmotic drag. Parameters governing liquid water formation and distribution in the cathode include the stoichiometry (or volumetric flow rate) of the inlet air, current density, cell temperature, and membrane water transport properties such as the diffusion and electro-osmotic drag coefficients.

The water flux to the cathode by diffusion, electro-osmosis, and hydraulic permeation can be expressed as

$$j_m = -D \frac{\Delta c_{c-a}}{\delta_m} + n_d \frac{I}{F} - \frac{K}{\mu_1} \Delta p_{c-a} \frac{\rho}{M_{H_2O}} \quad [1]$$

and

$$j_m \equiv \alpha \frac{I}{F} \quad [2]$$

where  $I$  is the current density,  $\rho$  the molar water density,  $\delta_m$  the membrane thickness,  $F$  the Faraday constant,  $K$  the hydraulic permeability,  $n_d$  the electro-osmotic drag coefficient of water,  $\mu_1$  the liquid water viscosity,  $D$  the diffusion coefficient,  $M_{H_2O}$  the molecular weight of water,  $\Delta c_{c-a}$  and  $\Delta p_{c-a}$  the water concentration difference and hydraulic pressure difference across the membrane, respectively.

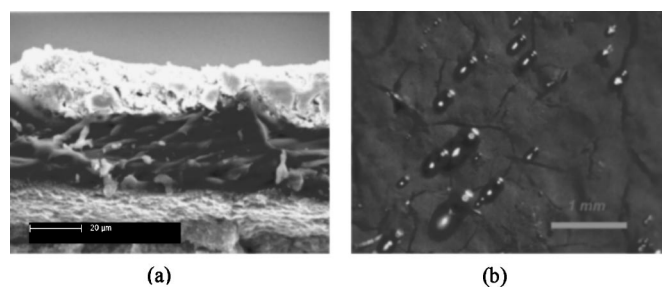


Figure 2. (a) SEM of the cross section of CCM, where the upper layer is the anode catalyst layer, the middle is Nafion membrane, and the bottom layer is the cathode. (b) Optical micrograph of the surface of microporous layer on carbon cloth.

The total rate of water arrival and production in the cathode is thus equal to

$$j_{H_2O} = \left( \alpha + \frac{1}{2} \right) \frac{I}{F} \quad [3]$$

Clearly, the three terms on the right side in Eq. 1 represent three modes of water transport through the membrane. The molecular diffusion is driven by the concentration gradient. The electro-osmotic drag is proportional to the current density, and the permeation flux is driven by the hydraulic pressure difference. The net water flux through the membrane can be conveniently quantified by a net water transport coefficient,  $\alpha$ , as defined in Eq. 2. This parameter, a combined result of electro-osmotic drag, diffusion, and hydraulic permeation through the membrane, dictates water management strategies in DMFC systems. For thick membranes such as Nafion 117,  $\alpha$  approaches the pure electro-osmotic drag coefficient as the other two modes of water transport are weakened with increasing membrane thickness.

From the viewpoint of water management in DMFCs, it is an ultimate goal to achieve  $\alpha$  values as low as possible or even negative. This requires increasing the hydraulic pressure in the cathode by using a hydrophobic GDL, as suggested independently by Peled *et al.*<sup>15</sup> and Pasaogullari and Wang.<sup>16</sup> The capillary pressure of the hydrophobic GDL in the cathode can be expressed as

$$p_c = p_g - p_l = 2\sigma \frac{\cos \theta_c}{r_c} \quad [4]$$

where  $\theta_c$  is the contact angle ( $>90^\circ$  for hydrophobic GDL) and  $r_c$  the pore radius. Thus the hydraulic pressure difference across the membrane for the liquid-feed DMFC is given by

$$\Delta p_{c-a} = p_l - p_a = (p_g - p_a) - 2\sigma \frac{\cos \theta_c}{r_c} \quad [5]$$

where  $p_a$  is the pressure in the anode. For a DMFC operating at the same pressure in both anode and cathode,  $p_g - p_a = 0$ . This makes the hydraulic pressure differential depend on the contact angle and pore radius of the cathode GDL, which can be enabled by a MPL design.

Equation 5 indicates that increasing the GDL hydrophobicity will result in a larger hydraulic pressure difference, leading to a lower  $\alpha$  value. However, excessive Teflon content in the MPL reduces the electrical conductivity and subsequently lowers cell performance. It is expected that there is an optimum hydrophobicity in the MPL for proper water management and improved performance. Equation 5 also indicates that a smaller pore radius gives rise to a larger hydraulic pressure difference, while a sufficiently reduced pore radius results in premature mass transport limitation in the cathode. Consequently, an increased air flow rate may be required to relieve this mass transport limitation, or pressurized oxygen may even be necessary, as demonstrated by Peled *et al.*<sup>15</sup> Unfortunately, using oxygen is not an option for portable DMFC systems.

Based on the above qualitative understanding of low- $\alpha$  mechanisms, a trial-and-error method has been carried out to fabricate low- $\alpha$  MEAs without compromising cell performance. Performance and water transport data of a representative MEA are presented in Fig. 3-5. Figure 3 shows the V-I polarization curves and power density curves at various temperatures. The concentration of the methanol solution is 2 M with flow rate of 0.08 mL/min, yielding a stoichiometry of 2 at 150 mA/cm<sup>2</sup>. Nonpressurized and nonhumidified air was fed into the cathode, with air flow rate of 54 SCCM, corresponding to a stoichiometry of 4 at 150 mA/cm<sup>2</sup>. The low flow rates of fuel and air at ambient pressure were intended to reduce power consumption by auxiliary pumps for portable applications. The polarization curves shown in Fig. 3 clearly display an activation region, an ohmic region and a mass transport limited region. Maxi-

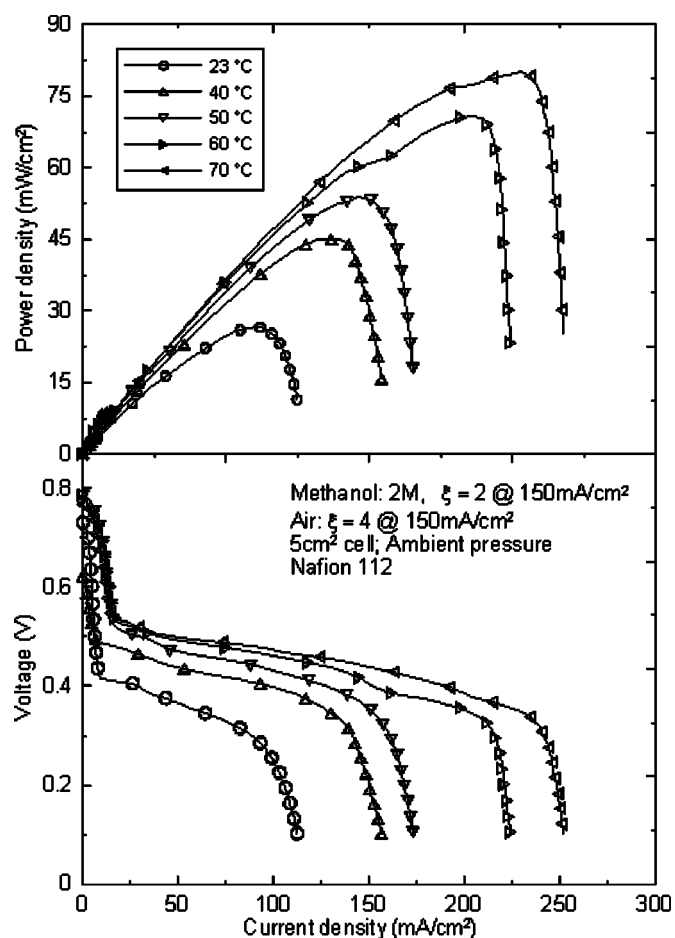


Figure 3. Current and power density curves at various temperatures with constant flow rates of methanol and ambient air.

mum power density reached  $26.5 \text{ mW/cm}^2$  at  $0.3 \text{ V}$  and room temperature ( $23^\circ\text{C}$ ),  $45 \text{ mW/cm}^2$  at  $0.36 \text{ V}$  and  $40^\circ\text{C}$ , and  $70.5 \text{ mW/cm}^2$  at  $0.36 \text{ V}$  and  $60^\circ\text{C}$ .

Figure 4 shows the evolution of cell voltage under a constant current load in a series of experiments measuring the net water

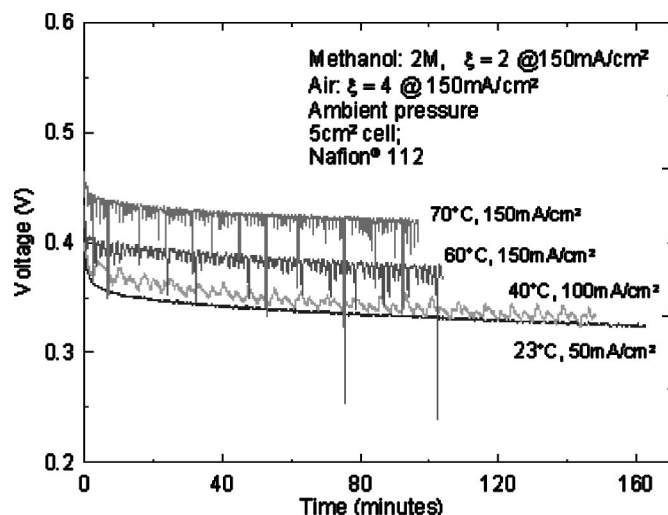


Figure 4. Evolution of the cell voltage during constant current loading in the measurement of the net water transport coefficient,  $\alpha$ .

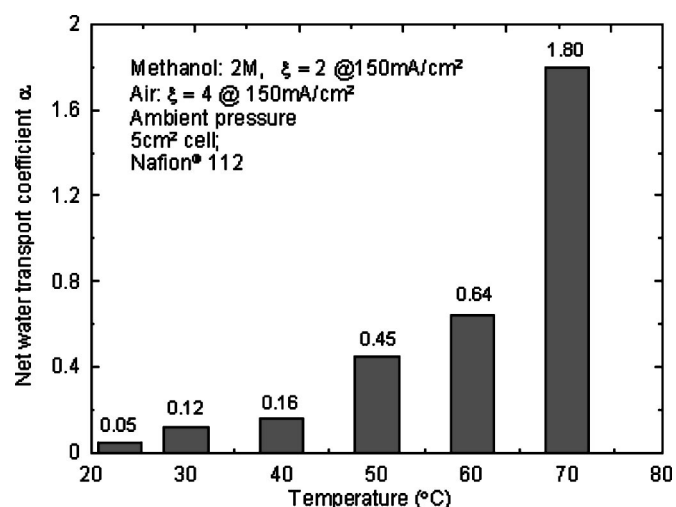


Figure 5. The net water transport coefficient,  $\alpha$ , at different temperatures with constant flow rates of methanol and ambient air.

transport coefficient,  $\alpha$ , at various temperatures using a moisture trap containing anhydrous calcium sulfate. The voltage suffers from an obvious drop at the beginning of each measurement. Subsequently, the voltage experiences a slight decay toward the end of each measurement. By intermittently stopping and restarting the liquid pump, cell performance can be restored. At small current densities, *e.g.*,  $50 \text{ mA/cm}^2$  at  $23^\circ\text{C}$  and  $100 \text{ mA/cm}^2$  at  $40^\circ\text{C}$ , cell voltage remains stable for an extended period of operation as shown in Fig. 4. At a higher current density of  $150 \text{ mA/cm}^2$  at  $60$  and  $70^\circ\text{C}$ , cell voltage occasionally experiences a sharp fluctuation when a slug of  $\text{CO}_2$  gas produced by the large current density blocks the anode channels temporarily, causing a short-lived mass transport limitation on the anode side. Careful attention to gas management<sup>18</sup> in the design of the anode flow field will likely remove this voltage oscillation. The steady-state power density at ambient pressure reached  $16 \text{ mW/cm}^2$  at  $23^\circ\text{C}$ ,  $33.3 \text{ mW/cm}^2$  at  $40^\circ\text{C}$ , and  $56 \text{ mW/cm}^2$  at  $60^\circ\text{C}$ , respectively.

Figure 5 displays the net water transport coefficient,  $\alpha$ , measured at different temperatures. Current density was measured at  $50 \text{ mA/cm}^2$  at  $23^\circ\text{C}$ ,  $65 \text{ mA/cm}^2$  at  $30^\circ\text{C}$ ,  $100 \text{ mA/cm}^2$  at  $40^\circ\text{C}$ ,  $125 \text{ mA/cm}^2$  at  $50^\circ\text{C}$ ,  $150 \text{ mA/cm}^2$  at  $60^\circ\text{C}$ , and  $150 \text{ mA/cm}^2$  at  $70^\circ\text{C}$ , respectively. Flow rates of methanol solution and air were fixed at the values given in Figs. 3 and 4. It is seen from Fig. 5 that the net water transport coefficient,  $\alpha$ , increases nearly exponentially with temperature. This is because the water vapor saturation pressure in the cathode increases sharply with temperature, thereby promoting water removal through the cathode air. It is seen from Fig. 5 that  $\alpha$  is only  $0.05$  at room temperature,  $0.16$  at  $40^\circ\text{C}$ , and  $0.64$  at  $60^\circ\text{C}$ , respectively. This  $\alpha$  range is significantly lower than the pure electro-osmotic drag coefficient. According to the experimental data,<sup>12</sup> the electro-osmotic drag coefficient  $n_d = 2.08$  at  $23^\circ\text{C}$ ,  $2.5$  at  $40^\circ\text{C}$ , and  $3$  at  $60^\circ\text{C}$ , respectively. Note that our method of measuring  $\alpha$  value included the water production from oxidation of crossover methanol at the cathode. Thus the true  $\alpha$  should be even smaller after subtracting water produced from oxidation of methanol that crosses from anode to cathode as in the Peled *et al.*<sup>15</sup> study.

Compared to the traditional use of a high air flow rate to prevent flooding and subsequent need for an external condenser to recover water from the cathode exhaust, this low- $\alpha$  feature enabled by a unique MEA design provides a simple way to reduce water loss from cathode exhaust, resulting in a more compact system by shrinking or eliminating the condenser. The anode does not require excessive water replenishment and allows the use of highly concentrated methanol fuel. Conversely, it is impossible to use concentrated fuel (*e.g.*,  $>3 \text{ M}$ ) even with an ideal membrane of zero

methanol crossover if the  $\alpha$ -value remains high (e.g., at 2.5). We have used commercially available Nafion membranes and MEA materials, and demonstrated that the cell produced reasonable performance with ambient air, while keeping the net water transport coefficient,  $\alpha$ , quite small.

Finally, methanol crossover is a concern for thin membranes such as Nafion 112 and should be addressed. Generally, the methanol crossover current density can be mathematically expressed by a simple relation between the crossover current,  $I_c$ , and anode mass-transport limiting current density,  $I_{A,lim}$ .<sup>13</sup> That is

$$I_c = I_{c,oc} \left( 1 - \frac{I}{I_{A,lim}} \right) \quad [6]$$

where  $I_{c,oc}$  is the crossover current density at open circuit, and  $I$  the operating current density. The anode limiting current density is about 225 mA/cm<sup>2</sup> at 60°C, as can be seen in Fig. 3. The crossover current density of the cell at open circuit was measured to be 157 mA/cm<sup>2</sup> using a MeOH anode vs. humidified N<sub>2</sub> cathode. According to Eq. 6, the crossover current densities at 150 and 200 mA/cm<sup>2</sup> are 52 and 17.4 mA/cm<sup>2</sup>, respectively. Thus, the fuel efficiency due to methanol crossover, defined as  $I/(I + I_c)$ , is equal to 74% at 150 mA/cm<sup>2</sup> and 92% at 200 mA/cm<sup>2</sup>.

### Conclusions

The hydraulic pressure buildup in the MPL of the cathode resulting from the large MPL contact angle and small pore size has been utilized to create a pressure differential across the membrane and hence water backflow from the cathode to anode. This approach substantially reduces water crossover through the membrane. Using a thin Nafion 112 membrane, a DMFC operating with ambient air has been demonstrated to yield a steady-state power density of 56 mW/cm<sup>2</sup> at 3.73 V and 60°C, with the net water transport coefficient 5-6 times smaller than the reported electro-osmotic drag coefficient and fuel efficiency between 74 and 92%. This low- $\alpha$  MEA design has the potential to eliminate or miniaturize the external condenser in a portable system. The reduced water loss from the anode also makes it possible to use concentrated methanol fuel. These

experimental results are useful for design of compact DMFC systems with high performance for portable application.

### Acknowledgments

This work was supported by DARPA Microsystem Technology Office (MTO) under Contract No. DAAH01-1-R001 and by industrial sponsors of ECEC.

The Pennsylvania State University assisted in meeting the publication costs of this article.

### References

1. G. Halpert, S. R. Narayanan, T. Valdez, W. Chun, H. Frank, A. Kindler, S. Surampudi, J. Kosek, C. Cropley, and A. LaConti, in *Proceedings of the 32nd Intersociety Energy Conversion Engineering Conference*, AIChE, p. 774 (1997).
2. S. Gottesfeld and M. S. Wilson, in *Energy Storage Systems for Electronics Devices*, T. Osaka and M. Datta, Editors, p. 487, Gordon and Breach Science Publishers, Singapore (2000).
3. S. R. Narayanan, T. I. Valdez, and N. Rohatgi, in *Handbook of Fuel Cells*, W. Vielstich, H. A. Gasteiger, and A. Lamm, Editors, p. 894, John Wiley & Sons Ltd., Chichester, England (2003).
4. A. S. Arico, S. Srinivasan, and V. Antonucci, *Fuel Cells*, **1**, 133 (2001).
5. C. Y. Wang, in *Handbook of Fuel Cells*, W. Vielstich, H. A. Gasteiger, and A. Lamm, Editors, p. 337, John Wiley & Sons Ltd., England (2003).
6. K. Scott, in *Handbook of Fuel Cells*, W. Vielstich, H. A. Gasteiger, and A. Lamm, Editors, p. 70, John Wiley & Sons Ltd., Chichester, England (2003).
7. G. Q. Lu, C. Y. Wang, T. J. Yen, and X. Zhang, *Electrochim. Acta*, **49**, 821 (2004).
8. S. R. Narayanan, H. Frank, B. Jeffries-Nakamura, M. Smart, W. Chun, G. Halpert, J. Kosek, and C. Cropley, in *Proton Conducting Membrane Fuel Cells I*, S. Gottesfeld, G. Halpert, and A. Landgrebe, Editors, PV 95-23, p. 278, The Electrochemical Society Proceedings Series, Pennington, NJ (1995).
9. X. Ren, T. E. Springer, T. A. Zawodzinski, and S. Gottesfeld, *J. Electrochem. Soc.*, **147**, 466 (2000).
10. J. T. Wang, S. Wasmus, and R. F. Savinell, *J. Electrochem. Soc.*, **143**, 1233 (1996).
11. A. Heinzl and V. M. Barragan, *J. Power Sources*, **84**, 70 (1999).
12. X. Ren and S. Gottesfeld, *J. Electrochem. Soc.*, **148**, A87 (2001).
13. G. Q. Lu and C. Y. Wang, in *Transport Phenomena in Fuel Cells*, B. Sundén and M. Fahgri, Editors, WIT Press, Billerica, MA (2004).
14. A. Blum, T. Duvdevani, M. Philosoph, N. Rudoy, and E. Peled, *J. Power Sources*, **117**, 22 (2003).
15. E. Peled, A. Blum, A. Aharon, M. Philosoph, and Y. Lavi, *Electrochem. Solid-State Lett.*, **6**, A268 (2003).
16. U. Pasaogullari and C. Y. Wang, *J. Electrochem. Soc.*, **151**, A399 (2004).
17. M. S. Wilson and S. Gottesfeld, *J. Appl. Electrochem.*, **22**, 1 (1992).
18. G. Q. Lu and C. Y. Wang, *J. Power Sources*, **134**, 33 (2004).